Development of Microfluidic Devices For In Situ investigation of Cells Using Surface-Enhanced Raman Spectroscopy

Yu-Han Ho

A thesis

submitted in partial fulfillment of the

requirements for the degree of

Master of Chemical Engineering

University of Washington

2015

Committee:

Qiuming Yu

Shaoyi Jiang

Francois Baneyx

Chemical Engingeering

University of Washington

Abstract

Development of Microfluidic Devices For In Situ investigation of Cells Using Surface-Enhanced Raman Spectroscopy

Yu-Han Ho

Chair of the Supervisory Committee:

Qiuming Yu

Chemical Engineering

Surface-enhanced Raman spectroscopy (SERS) has immerged as a power analytical and sensing technique for many applications in biomedical diagnosis, life sciences, food safety, and environment monitoring because of its molecular specificity and high sensitivity. The inactive Raman scattering of water molecule makes SERS a suitable tool for studying biological systems. Microfluidic devices have also attracted a tremendous interest for the aforementioned applications. By

integrating SERS-active substrates with microfluidic devices, it offers a new capability for in situ investigation of biological systems, their dynamic behaviors, and response to drugs or microenvironment changes. In this work, we designed and fabricated a microfluidic device with SERS-active substrates surrounding by cell traps in microfluidic channels for in situ study of live cells using SERS. The SERS-active substrates are quasi-3D plasmonic nanostructure array (Q3D-PNA) made in h-PDMS/PMDS with physically separated gold film with nanoholes op top and gold nanodisks at the bottom of nanowells. The Q3D-PNAs with the strongest local electric fields (hot spots) at the top and bottom water/Au interfaces, designed by 3D finite-difference time-domain (3D-FDTD) electromagnetic simulations, were placed at the up and down stream of the microfluidic channel for sensitive analysis of cells and small components, respectively. The microfluidic device was fabricated via soft lithography. We demonstrated that normal (COS-7) and cancer (HpeG2) cells were captured on the Q3D-PNAs and investigated in situ using SERS.

Introduction

Raman scattering, discovered by C. V. Raman in 1921, is an inelastic scattering with the energy difference of the incident and emission photons corresponding to the change of vibrational states of a molecule. There is only a small fraction of incident photons scattered by Raman scattering so the intensity of Raman

signals is usually very weak even though a laser is used to excite this process. In the early 70s, it was found that when molecules adsorbed on roughen silver surfaces, their Raman signals were enhanced significantly[1]. This phenomenon is called surface-enhanced Raman scattering (SERS). It has been known that SERS is due to both electromagnetic and chemical enhancements. The electromagnetic enhancement is dominated and is typically in the order of 10^6-10^7, which is resulted from the extremely concentrated local electric fields (hot spots) in the vicinity of nanostructured noble metal surfaces caused by localized surface plasmon resonance (LSPR). The chemical enhancement is typically in the order of 10^2, which is caused by possible resonant electron transfer between adsorbed molecules and the nanostructured metal surfaces.

Recently, SERS has been recognized as a powerful technique for chemical and biological sensing because of many advantages it offers, such as molecule-specific fingerprints without labeling, narrow resolved bands of signals, and ultra-high sensitivity. The inactive Raman vibrational mode of water molecule makes SERS a powerful tool to study biological system. However, SERS is a near-field effect, which means that analytes are either on or close to the metal surface, then their Raman scattering can be enhanced. While this effect could be a drawback of SERS technique, it also provides a way to preferentially detect molecules or the outer most cell membranes directly attaching on the metal surface. Unlike commonly used

silver or gold nanoparticles as SERS-active substrates which are difficult to control the uniformity and intensity of hot spots, SERS-active substrates made of metal-dielectric nanostructures can be rationally designed to achieve strong enhancement with a desired excitation laser and highly uniformly distributed hot spots to enable sensitive and reproducible measurements. For example, quasi-3D plasmonic nanostructure arrays (Q3D-PNAs), composed of physically separated gold thin film with nanoholes on top and gold nanodisks at the bottom of nanowells, offer large tunability of plasmonic properties. In the past several years, our group has systematically investigated Q3D-PNAs with various shapes, dimensions and dielectric materials as SERS-active substrates[3-7]. Both the intensity of local electric field and the position of the strongest local electric field, i.e., hot spots, can be tuned by simply varying the diameter of nanoholes of Q3D-PNAs[3]. Marine pathogenic bacteria were rapidly identified with SERS barcodes generated by using the Q3D-PNA SERS-active substrate with hot spots on the top Au/air interface where bacteria attached[4]. Q3D-PNAs can be made on a silicon substrate or an indum tin oxide (ITO) coated glass substrate via electron beam lithography (EBL), or in polydimethylsiloxane (PDMS) and polyurethane (PU) via soft lithography, or in silicon via EBL followed by reactive ion etching (RIE) [5]. Plasmonic properties and SERS effect are very sensitive to the surrounding dielectric materials. Making Q3D-PNAs in PDMS not only offers a cost effective way to produce highly sensitive and

reproducible SERS-active substrates, but also makes it possible to integrate SERS-active substrates with microfluidic systems to enable in situ detection. Strong and reproducible SERS signals of 4-mercaptopyridine (4MP) were shown on the substrates with Q3D-PNAs made of PDMS via soft lithography[6]. Furthermore, an optofluidic system with Q3D-PNAs in PDMS was made and the capability of online SERS detection of malathion as well as the improvement of detection sensitivity via increasing the flow rate were demonstrated[7].

There are more and more research of SERS application recently in various way based on solving its shortcoming of requiring samples close for enhancement because it has powerful capability of doing chemical and biological detection. The most common way is using metal nanoparticles like Ag or Au particles aggregating together to produce a lots of gaps for generating SERS effect.[8-11] Some of them demonstrate functionalized Ag/Au nanoparticles as probes for SERS detection while them attaching to specific cells[8]. Nevertheless, SERS effect factor is usually low with those nanoparticles enhancing methods comparing to nanostructures arrays of SERS substrates. With applying nanostructure array of SERS, another type of SERS applications is functionalizing SERS substrates with antibiotic or other chemicals for capturing bacteria or some other bio-sample via chemical bond while flowing medium composed of complex component like human blood through the substrates[12]. This type of method solved the shortcoming of nanostructure arrays of SERS

substrate that it always needs samples to attach closely on substrate surfaces for enhancing Raman signals. However, this functionalizing method can only be employed for the samples having specific functional group to bind. Recently, researchers develop a microfluidic system employing different diffusivities of particles sizes for separating target molecules such as methamphetamine from complex medium like human blood, then apply Ag particles that molecules can attach to for enhancing Raman signals[13]. This method has the problem of weaker enhancement comparing to nanostructure arrays of SERS substrates as well. On the other hand, cell traps designed in microfluidic devices for capturing cells mechanically is also demonstrated in some researches[14-18], for observing the dynamic metabolism of cells, analyzing inner components of cells or separating specific cells from complex medium.

In this paper, we designed and fabricated microfluidic devices by integrating Q3D-PNAs surrounded with cell trapping structures for in situ investigation of cells using SERS. Two sets of Q3D-PNAs were designed using 3D finite-difference time-domain (3D-FDTD) electromagnetic simulations with the goal to yield the strongest local electric fields at the top and bottom water/gold interfaces in order to sensitively analyze cell membranes and small molecules, respectively. The Q3D-PNAs with the hot spots on top were placed in the upstream of the microfluidic channel and each of them was surrounded by a micron-scaled cell trapping structure with an opening

facing the flow direction in order to capture cells from the suspension flowing through the microfluidic channel. The Q3D-PNAs with the hot spots at the bottom were placed in the downstream of the microfluidic channel in order to analyze small molecules in the suspension. A silicon master mold with protruded nanopillars and microfluidic channels and microhole for cell trapping structures were prepared via multi-scale, multi-step fabrication including EBL, photolithography, and RIE. Soft lithography was utilized to fabricate the h-PDMS/PDMS composite chip containing nanohole array surrounded by micron-scale protruded cell trapping structures in microfluidic channels. The h-PDMS/PDMS chip was bounded with a piece of cover glass slide to form a microfluidic device with Q3D-PNA SERS-active substrates in channels. The performance of the SERS microfluidic device was evaluated using 4-mercaptobenzoic acid (4-MBA) on Q3D-PNAs. Cell trapping and in situ analysis of cells were demonstrated using African green monkey's kidney cells (COS-7) and human liver cancer cells (HepG2).

Materials and methods

Materials

Trichloro (1H, 1H, 2H, 2H-perfluorooctyl) silane, (3-Mercaptopropyl)trimethoxysilane (MPTMS) and Sylgard 184 PDMS kit were purchased from Sigma-Alorich. For making h-PDMS, (7.0-8.0%

vinylmethylsiloxane) - dimethylsiloxane copolymer (h-PDMS copolymer, VDT-731), platinum catalyst (SIP6831.2), 1,3,5,7-teravinyl-1,3,5,7-tetramethylcyclotetrasiloxane (modulator, SIT7900.0), and methylhydrosiloxane copolymer (cross-linker, HMS-301) were purchased from Gelest.

Design of Q3D-PNAs in PDMS using FDTD simulations

The Finite-Difference Time-Domain (FDTD) method was used to design the Q3D-PNAs with spatial control of the electromagnetic hot spots, and to investigate the electric field distributions of the nanostructures. Q3D-PNAs were optimized as a function of nanohole diameter, pitch, depth of the PDMS nanocavity and gold film thickness. The unit cell for the simulations consisted of a single plasmonic nanohole. Boundary conditions were set to periodic in both the x and y directions, and a perfectly matched layer (PML) condition was set in the z-direction. The simulation volume was extended to 400 nm above the top gold film, and 400 nm below the gold nanodisk. To help resolve the sharp contrast of the gold/PDMS and gold/water interfaces, a non-uniform mesh was used throughout the simulation volume. Additional meshing was added around the perforated gold film and gold nanodisk to help visualize the electric field profiles. This meshing extended 10 nm above and 10 nm below each gold structure, with a resolution of 2 nm in all three spatial dimensions. A plane wave was used as the radiative source. The plane wave was

impinged normal to the gold surface from a distance of 300 nm, and was polarized with the electric field component in the x-direction. The background refractive index was set to n = 1.33 to replicate an aqueous environment. Refractive indices for the gold film and PDMS nanostructures were taken from previously reported values[26]. Electric field profiles were visualized by placing power monitors on the surfaces of both the perforated gold film and the gold nanodisk in the xy-plane, as well as through the center of the nanohole in the xz-plane.

Design of microfluidic devices with Q3D-PNAs and cell traps

The layout of four microfluidic chips designed on a 4-inch silicon wafer is as shown in Fig. 1(a). Three of them have two individual channels, one with three inlets and another with one inlet (Fig. 1(b)). The same layout of Q3D-PNAs was designed in all these channels. As shown in Fig. 1(c), ten Q3D-PNAs with the hot spots at the water/Au interfaces on top and bottom were placed at the up- and down-stream of the microfluidic channel, respectively. The dimensions of these two types of Q3D-PNAs designed by FDTD simulations are shown in Fig. 1(d) and (e), respectively. The depth of the nanowell was fixed to be 300 nm (Fig. 2). In each of the three chips with the same microfluidic channel design, three different cell trap structures shown in Fig. 1 (f)-(h) were designed to surround the Q3D-PNAs. The channel width, depth and length are 200 μm, 30 μm and 13.65 mm, respectively, and the diameter of the

inlet/outlet is 4 mm. The Q3D-PNA is typically 18 μm x 18 μm. The cross-section view of the nanopillars, channel and cell trap of the silicon master mold is shown in Fig. 2(a). Top and cross-section views of a Q3D-PNA surrounded by a cup-like cell trap in microfluidic channel in an h-PDMS/PDMS composite chip ae shown in Fig. 2(b).

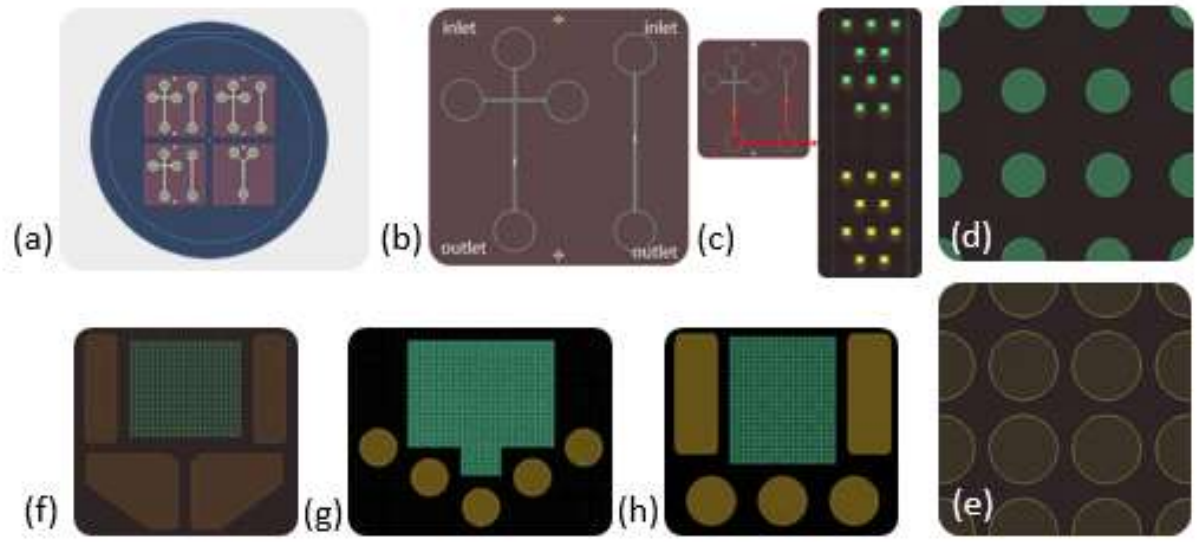

Figure 1. (a) Layout of four pieces of microfluidic chips on a 4-inch silicon wafer. (b) Two types of flow channels on three of four chips, one with three inlets and another with one inlet. Each of the three chips has the same layout of Q3D-PNAs but different types of cell traps shown in (f)-(h). (c) Ten Q3D-PNAs with the hot spots on top and at the bottom are placed at the upstream and downstream of the microfluidic channel, respectively. (d) The Q3D-PNA with the hot spots on top. (e)

The Q3D-PNA with the hot spots at the bottom. (f) A cup-like cell trap. (g) A pachinko-like cell trap. (h) A mixing style cell trap.

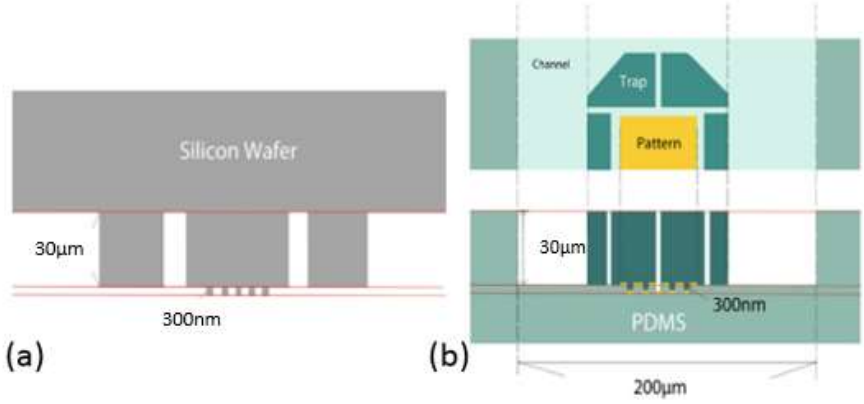

Figure 2. (a) Cross-section view of the silicon master. (b) Top and cross-section views of a Q3D-PNA surrounded by a cup-like cell trap in microfluidic channel in an h-PDMS/PDMS composite chip.

Fabrication of h-PDMS/PDMS composite microfluidic devices

The fabrication procedure of silicon master mold is shown in Fig. 3. One silicon master mold for soft lithography was made on a 4-in silicon wafer with the design shown in Fig. 1. The silicon nanopillar arrays were fabricated first using EBL followed by RIE and then, the microfluidic channels and the cell traps were fabricated using photolithography followed by RIE.

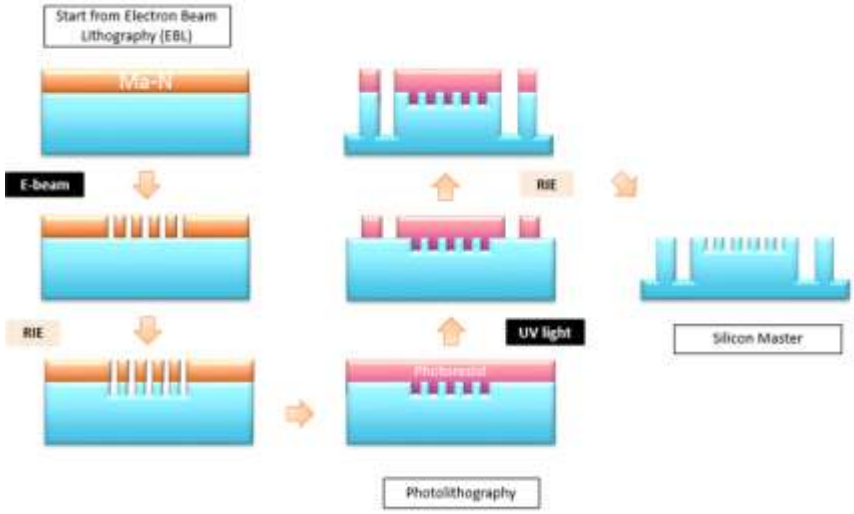

Figure 3. The procedure to make a silicon master mold via nano- and micro-fabrication involing EBL, photolithography, and RIE.

Figure 4 shows the procedure to make microfluidic devices. The silicon master mold was exposed to oxygen plasma for 5 min and then silanized by placing

the wafer in a vacuum desiccator with a drop of trichloro (1H, 1H, 2H, 2H-perfluorooctyl) silane for 1 h. The hydrophobic anti-adhesive silane monolayer was formed on the surface of the master mold. For soft lithography, an h-PDMS thin film was first coated on the mold to transfer the nanoscaled holes[7]. h-PDMS was the mixture composed of 3.4 g of vinylmethylsiloxane copolymer (VDT-731), 0.1 g of modulator, 18 μl of platinum catalyst and 1 g of methylhydrosiloxane copolymer[22]. These four ingredients were mixed well by stirring at room temperature for 1 min, the solution was spin coated on the silanized silicon master mold at 1000 rpm for 60 s. The coated h-PDMS was cured at 60 ℃ for 10 min. Next, a regular PDMS mixture containing the PDMS base copolymer and the cross-linker with a ratio of 10:1 was poured over the h-PDMS coated mold in a petridish. After degasing for 30 min in a vacuum desiccator, the h-PDMS/PDMS was cured at 70 ℃ for 6 h. The h-PDMS/PDMS composite piece was easily released from the silicon mold because of the hydrophobic anti-adhesive silane layer on the silicon surface. The h-PDMS/PDMS was cut into four microfluidic chips.

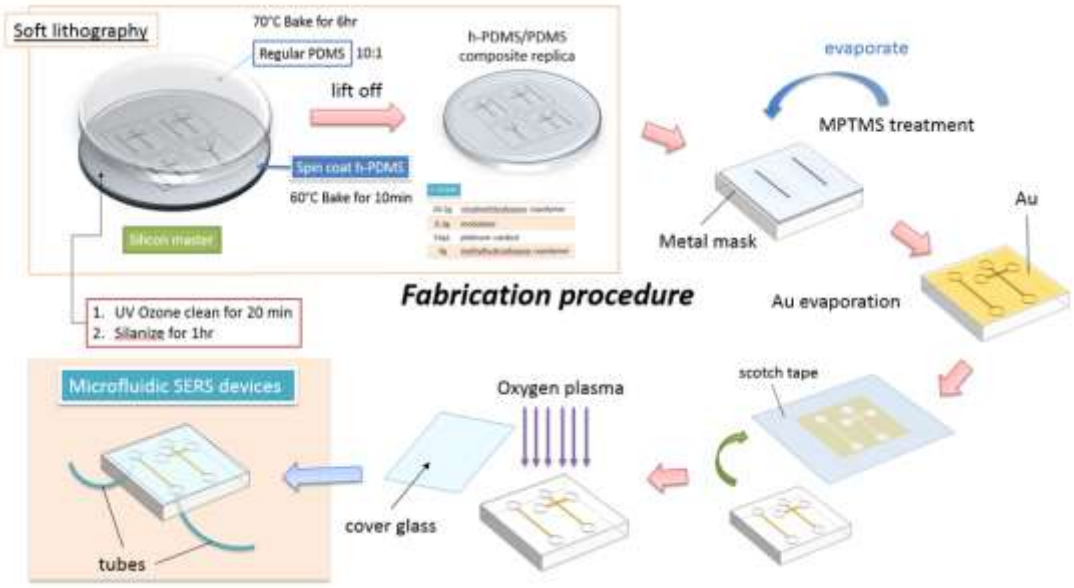

Figure 4. The procedure to an h/PDMS/PDMS microfluidic device involing soft lithography, gold deposition, and bonding the chip with a cover glass slide.

In order to improve the adhesion and the smoothness of gold thin film on h-PDMS/PDMS, the h-PDMS/PDMS surface was treated with MPTMS. To do so, the h-PDMS/PDMS surface was first oxidized by putting the chip in an UV/ozone cleaner for 20 min. Then, a monolayer of MPTMS was formed on the oxidized h-PDMS/PDMS surface following the same method as aforementioned silanization for 2 h. The h-PDMS/PDMS surface was covered with tapes except the channels during the MPTMS treatment and then peeled off afterwards. A 50 nm gold film was deposited on the MPTMS treated h-PDMS/PDMS surface using a thermal evaporator. The gold film outside the channels was peeled off simply using a scotch

tape because of the weak adhesion of gold on h-PDMS/PDMS without the MPTMS monolayer.

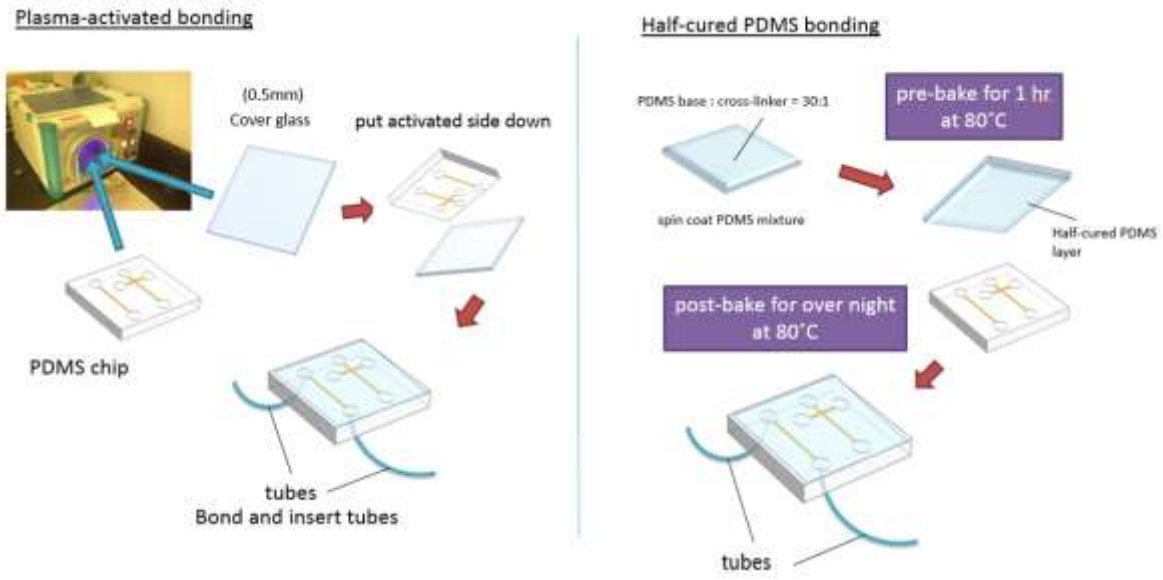

Figure 5. An illustration showing two methods used in bonding the h-PDMS/PDMS chip with a cover glass slide.

Two methods were used to bond the h-PDMS/PDMS chip to a cover glass slide to form a microfluidic device as illustrated in Fig. 5. One method was to expose both the h-PDMS/PDMS surface and the cover glass slide surface to oxygen plasma in an oxygen plasma cleaner under 100 W for 5 min and then to press them together. Another way was to use a half-cured PDMS on a cover glass slide to seal the h-PDMS/PDMS microfluidic channels[27]. A mixture of the PDMS base polymer and the cross-linker in a ratio of 30:1 was mixed well and then spin coated on a cover

glass slide at 4000 rpm for 60 s. Pre-bake the cover glass slide with the extremely thin soft PDMS layer at 80˚C for 1 h to yield a half-cured PDMS layer on the cover glass slide. Put this cover glass slide onto the h-PDMS/PDMS composite chip, fixed them with two glass slides, clamped them together with clips, and then baked in an oven at 80 ℃ for overnight until the half-cured PDMS adhesive layer was totally cured. The inlet/outlet areas were punched holes with a hole puncher and tubes were inserted and sealed with PDMS. One assembled h-PDMS/PDMS microfluidic device is shown in Fig. 6

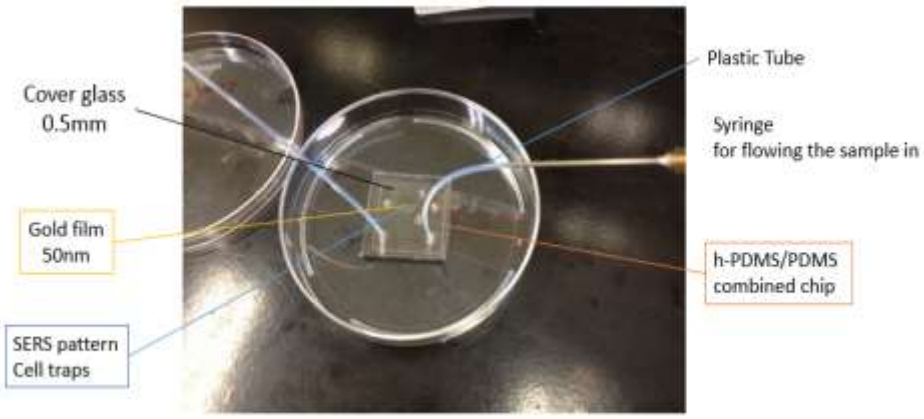

Figure 6. A photo of a fabricated microfluidic device.

Culturing of COS-7 and HepG2 cells

To culture COS-7 and HepG2 cells, 1 ml of frozen cell line in DMSO solution was taken and deforested in 40˚C water bath for a short time. Add 10ml of cell culture media (DMEM with 10% FBS) into the 40˚C water bath to keep cells in an appropriate environment. After the pre-heating procedure was done, drop the cell line solution in 10 ml of cell culture media and centrifuge at 1000 rpm for 5 min to separate DMSO from cells since DMSO is toxic to cells. Discarded the supernatant containing DMSO and kept the membrane-like thin cell layer at the tube bottom. To the tube, added 9 ml of fresh cell culture medium, shook to redisperse cells in the fresh medium, transferred the solution to a cell culture container, and then put the container in an incubator at 37˚C with 5% CO_2.

To passenger cells, prepare DMEM (with 10% FBS), DPBS, trypsin in 40˚C water bath in order to keep cells always in appropriate condition during the passenger process. Trypsin can digest proteins on cell wall and makes them detached from substrates. DPBS is used for washing away the proteins on surfaces of cells before adding trypsin. Took the cell culture container out of the incubator, poured the medium out, added 2 ml of DPBS, shook the container for finely washing cells on substrates, and then extracted DBPS out with pipet. Added 1 ml of trypsin to rinse cells, discarded the trypsin, and put the container back to the incubator for 5 min. The small amount of trypsin left around cells is enough to digest proteins on cell walls and make cells to detach. All cells were floating instead of attaching to the

container bottom by viewing under microscope. Added 5 ml of medium in the cell container, then extracted 4 ml of the medium, added another 4 ml of fresh medium into the container, and then put the container back to the incubator. Repeated this procedure in 4-5 days later. The extracted 4 ml of cell culture medium was full of live cells and can be used as a sample solution for SERS experiments.

SERS measurements

All Raman spectra were acquired on Renishaw InVia Raman spectrometer with Leica DMLM upright microscope attached. 4-MBA was used as a test sample to evaluate the enhancement of Q3D-PNAs in microfluidic channels. A 0.1 mM of 4-MBA aqueous solution with 10% alcohol was slowly injected into a channel using a syringe for 10 s. The 4-MBA solution was kept in the channel for 2 h before taking Raman spectra. Raman spectra were taken using a 785 nm excitation laser through a 50X (N.A. = 0.8) lens to focus the laser spot (2.5 μm x 20 μm) on the Q3D-PNA patterns through the cover glass slide. The laser power was 0.5% of the full power, CCD exposure time was 20 s and the accumulation was 5 times.

To avoid the interference of cell culture medium in taking SERS signals of cells, the 4 ml of cell culture medium containing COS-7 cells was centrifuged at 1000 rpm for 5 min. Discarded the supernatant and added 4 ml of DMEM without phenol red to redisperse cells. A 0.5 ml of cell solution was slowly injected into a

microfluidic channel using a syringe and incubated for 1 h to let cells attach to the Q3D-PNAs before taking Raman spectra. Raman spectra were taken at three different places on each Q3D-PNA pattern. Raman spectra of cells were taken using a 785 nm excitation laser through a 50X (N.A. = 0.8) lens to focus the laser spot (2.5 μm x 20 μm) on a cell on the Q3D-PNA pattern through the cover glass slide. The laser power was 0.5% of the full power, CCD exposure time was 20 s and the accumulation was 5 or 10 times. The same procedure was applied to take the SERS spectra of HepG2 cells. Data was analyzed using the software WiRE™ with the Renishaw instrument.

Results and discussion

Q3D-PNAs designed by FDTD simulations

The Q3D-PNAs made in PDMS were designed using FDTD electromagnetic simulations with the goal to yield the hot spots at the top and bottom water/Au interfaces, respectively. The diameters of 350 and 450 nm and the pitches of 687 and 550 nm were determined for the Q3D-PNAs with the hot spots at the top and bottom water/Au interfaces, respectively. All two types of patterns have the same depth of 300 nm. Figure 7 shows the FDTD simulated electric filed distributions of the hot spots at the top (Fig. 7(a)) and bottom (Fig. 7(b)). The electromagnetic enhancement factor (EF) was calculated using the expression of the forth power of the ratio of the strongest local electric field to the incident electric field $(E_{max}/E_0)^4$ and the results

of $1.15x10^{-5}$ and $3.2x10^{-5}$ were obtained for hot spots at the water/Au interfaces on top and bottom, respectively. The strongest local electric fields can be seen as bright spots at the top (Fig. 7(a)) or at the bottom (Fig. 7(b)) of the water/Au interface.

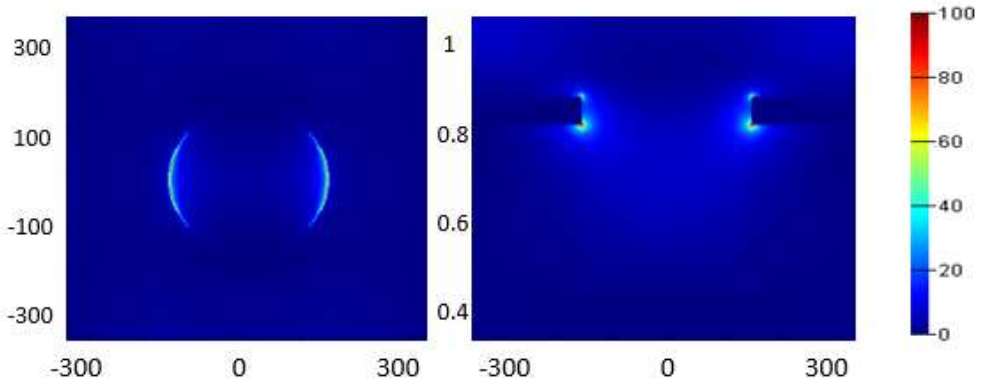

(a)

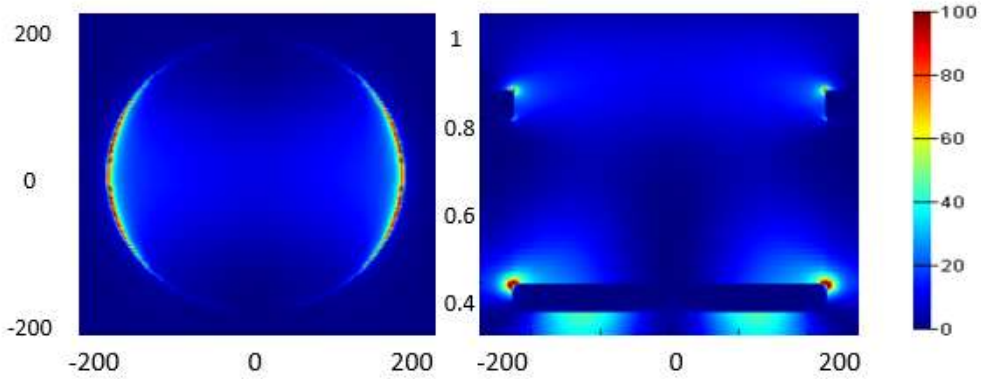

(b)

Figure 7. Top and cross-section views of FDTD simulated electric field distributions. The Q3D-PNA with hot spots at the top (a) and bottom (b) water/Au interfaces. The scale bar is $(E/E_0)^2$.

Q3D-PNAs in microfluidic channels

The silicon master mold was fabricated using multiple-step nano/microfabrications as illustrated in Fig. 3. Figure 8(a) shows the SEM image of

a microfluidic channel on the silicon master mold with ten Q3D-PNAs with the hot spots on top and ten Q3D-PNAs with the hot spots at the bottom. The Q3D-PNAs with hot-spots on top (Fig. 8(b)) are placed at the upstream of the channel for detecting cells. To ensure cells to be trapped on the places with Q3D-PNAs, cell traps were made surrounding Q3D-PNAs for capturing and fixing cells. Three types of cell traps (Fig. 1(f-h)) were designed to evaluate the effecy of cell trapping. To prevent cells flow over the cell traps, all cell traps are designed to have a height of 30 μm. The Q3D-PNAs with hot-spots at bottom (Fig. 8(c)) are placed at the downstream of the channel for detecting small molecules or proteins. The SEM images of Q3D-PNAs with a cup-like and a pachinko-like cell cell traps are shown in Fig. 8(d) and (e), respectively.

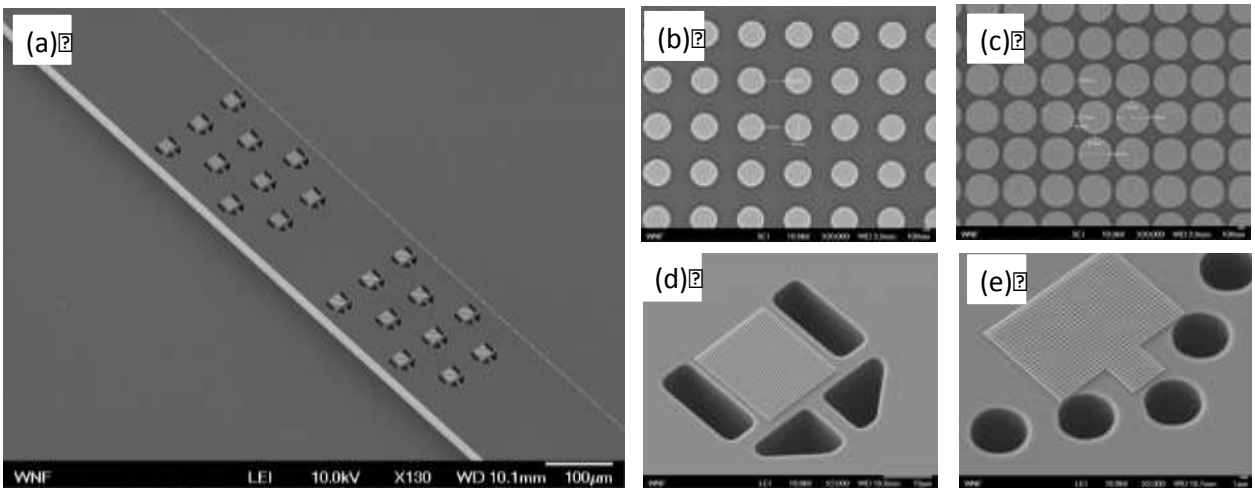

Figure 8. SEM images of the silicon master mold. (a) One channel; (b) Q3D-PNA with hot spots on top; (c) Q3D-PNA with hot spots at bottom; (d) A cup-like cell trap surrounding a Q3D-PNA; (e) A pachinko-like cell trap surrounding a Q3D-PNA.

The h-PDMS/PDMS micrifluidic chips were made via soft lithography. The procedure is shown in Fig. 4. The SEM images of Q3D-PNAs with the hot spots on top and at bottom made in h-PDMS/PDMS composite chip covered with a 50 nm gold layer are shown in Fig. 9(a) and (b), respectively. The nanohole arrays were successfully made in h-PDMS/PDMS with sharp edge and uniform size. Figure 9(c-e) show the SEM images of three different cell traps surrounding Q3D-PNAs. The micro-scale traps were also successfully made in h-PDMS/PDMS although some defects are observed, which may be caused by not fully silaniized silicon surface in the deep micro-scale holes.

(a) 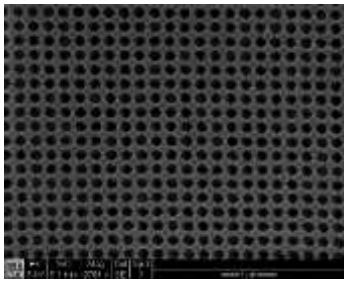 (b) 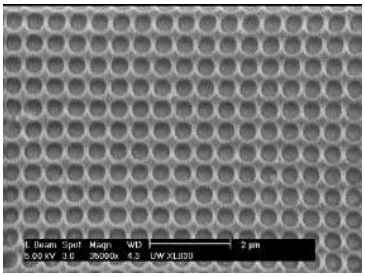

(c) 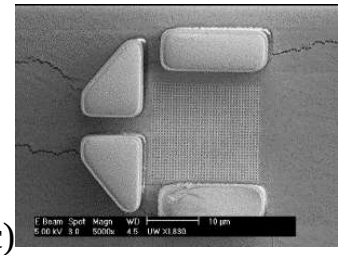 (d) 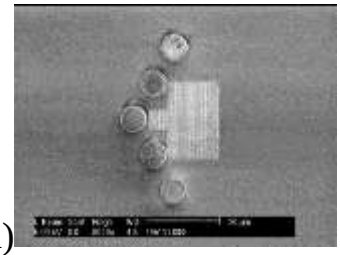 (e) 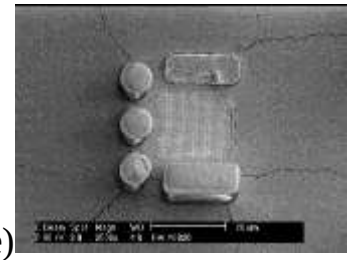

Figure 9. (a) and (b) SEM images of the Q3D-PNAs with hot spots at the interface of water/Au on top and at bottom, respectively. (c-e) SEM images of cup-like, pachiko-like, and mixed-style cell traps surrounding Q3D-PNAs, respectively.

Silanization of the silicon master mold surface is a critical step in soft lithography in order to prevent h-PDMS/PDMS from sticking on the silicon master mold surface. Trichloro (1H, 1H, 2H, 2H-perfluorooctyl) silane is commonly used for this purpose because of its two functional end groups -$SiCl_3$ and -CF_3. Silicon surface has a thin layer of naturally oxidized layer, which turns to be terminated with -OH groups after exposed to oxygen plasma. The –OH groups can easily react with -$SiCl_3$ and a self-assembled monolayer (SAM) can be formed on the silicon master mold surface. The other tail of this organosilane, -CF3, is exceptional hydrophobic, making the silicon master mold surface extremely anti-adhesive while h-PDMS/PDMS was casted.

Another challenge to be tackled is to make a smooth, stable gold layer on h-PDMS/PDMS. The bonding strength between Au and h-PDMS/PDMS is weak. Even a lightly bending of an h-PDMS/PDMS chip can cause cracks on Au film. To ensure the stability of Q3D-PNAs for in situ SERS measurements in microfluidic channels, the bonding of Au to h-PDMS/PDMS was improved by forming a SAM of MPTMS because of its two functional groups -OCH_3 and –SH. Similar to the

silanization process, MPTMS can form a SAM via -OCH_3 group to the –OH groups at the h-PDMS/PDMS surface after exposure to oxygen plasma[20]. The –SH group on the other end can improve the bonding strength to gold by forming a S-Au bond during gold deposition. The optical images in Fig. 10(a) and (b) clearly show the difference of Au films deposited on h-PDMS/PDMS chips with and without MPTMS treatment. The Au surface is much smoother with less cracks for the h-PDMS/PDMS treated with MPTMS before gold deposition.

(a) 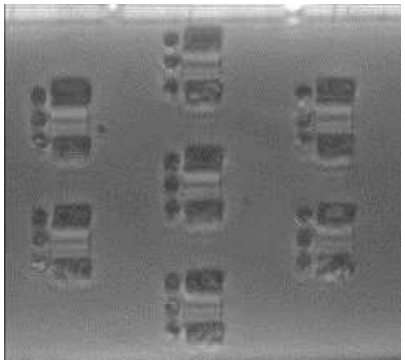 (b) 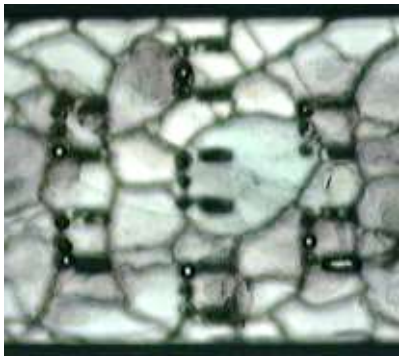

Figure 10. Optical images of Au films deposited on h-PDMS/PDMS with (a) and without (b) MPTMS treatment of the h-PDMS/PDMS surfaces before gold deposition.

To bond the h-PDMS/PDMS chip to a cover glass slide, two methods were used in this work. The first method utilizes oxygen plasma to activate both h-PDMS/PDMS and cover glass slide surfaces. The h-PDMS surface is oxidized with oxygen plasma, where the hydrocarbons are etched following by silanol groups left.

This makes h-PDMS surface extremely hydrophilic. Oxygen-treated cover glass slide was placed in contact with the oxidized h-PDMS to form the Si-O-Si bond that can permanently seal the h-PDMS/PDMS chip and the cover glass slide together. One thing to be aware of is that both the h-PDMS/PDMS and cover glass slide surfaces have to be very clean to ensure the success of bonding. Even invisible tiny dusts could ruin this bonding process. To make clean surfaces, both h-PDMS/PDMS chip and cover glass slide were pre-cleaned in UV ozone cleaner for 20 min. The second method to seal the h-PDMS/PDMS chip with a cover glass slide was adopted from the method of multilayer soft lithography for fabricating complex microdevices [16]. In this method, the mixture of the PDMS copolymer and the cross-linker with a ratio of 30:1 was spin coated on a cover glass slide. With less portion of cross-linker, the PDMS is softer and hard to cure. The half-cured thin layer of PDMS on the cover glass side can stick to the h-PDMS/PDMS surface when the PDMS is fully cured after postbaking.. The advantages of this method are that there is no need to treat the h-PDMS/PDMS surface with oxygen plasma and the sealing still works even the h-PDMS/PDMS surface is not very clean.

Trapping cells with the use of microfluidic devices has been explored for various applications[14-18]. For example, a cup-like trapping structure was used for trapping cells that have uptaken silver nanoparticles functionalized with Raman-tag molecules for SERS mapping of cells[14]. Another cell trapping method was

demonstrated by using micro-patterned sensors and cell self-assembly for measuring the oxygen consumption rate of single cells[15]. They also made cup-like traps on a glass substrate with oxygen sensor around for trapping cells. To enhance the possibility of cell trapping, they exploit the centrifugal forces to pull the cells toward the glass surface by spinning the substrate in centrifuge so that those cup-like traps on the glass surface can trap the cells much easier. Pachinko-like cell traps were placed in microfluidic channels to trap cancer cell from human blood and then to collect cancers by reversing flow[16]. In this work, three types of cell traps were designed in order to capture various cells or bacteria. The cup-like trap was designed for trapping cells that are not rigid and can deform easily by fluidic pressure. In this case, the gap between each piece of the trap needs to be small, otherwise, cells can be squeezed out of the traps. The potential drawbacks are the difficult of sample solution flowing through these gaps and the difficult in fabricaiton because of the high aspect ratio. The pachiko-like trap was designed for capturing rigid larger cells such as cancer cells. The mixing type trap with both the features of cup-like and pachinko-like traps was designed to solve the potential shortcomes of those two types of traps.The height of cell traps is the same as that of the channel to prevent cells from escaping by floating up over the traps.

Evaluation of SERS performance of Q3D-PNAs in microfluidic channels

The SERS performance of Q3D-PNAs made in h-PDMS/PDMS microfluidic channels was evaluated using 4-MBA, the molecule has been commonly used as a SERS reporter in many studies because it has large Raman scattering cross-section and can form SAM on Au surface[23,24]. Figure 11 shows the SERS spectrum of 4-MBA taken from one Q3D-PNA pattern after the 4-MBA solution was injected and incubated for 2 h. Two strong peaks were observed at 1078 and 1589 cm^{-1} due to C-C ring-breathing modes. The -CH band was observed at 1179 cm^{-1}. High reproducibility of SERS spectra taken on Q3D-PNAs is demonstrated in Fig. 12. SERS spectra were taken from the Q3D-PNAs with the hot spots on top and bottom and each from three different patterns. All the spectra are identical in terms of the peak position, shape and intensity, indicating high reproducibility.

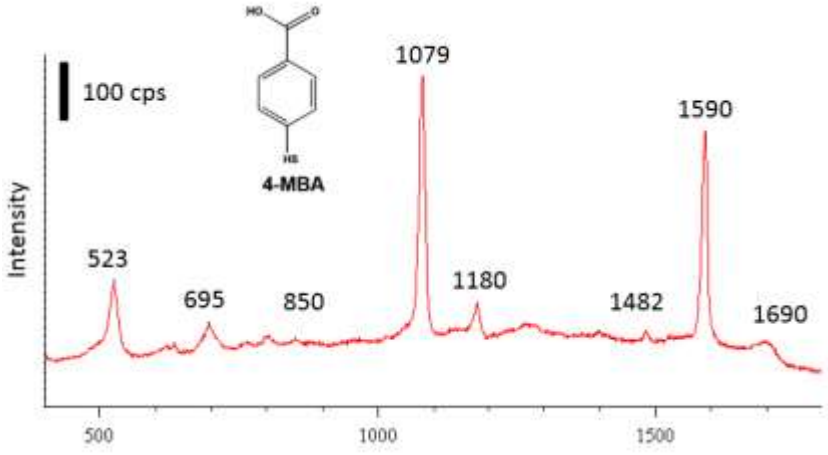

Figure 11. SERS spectrum of 4-MBA SAM taken in situ on one Q3D-PNA.

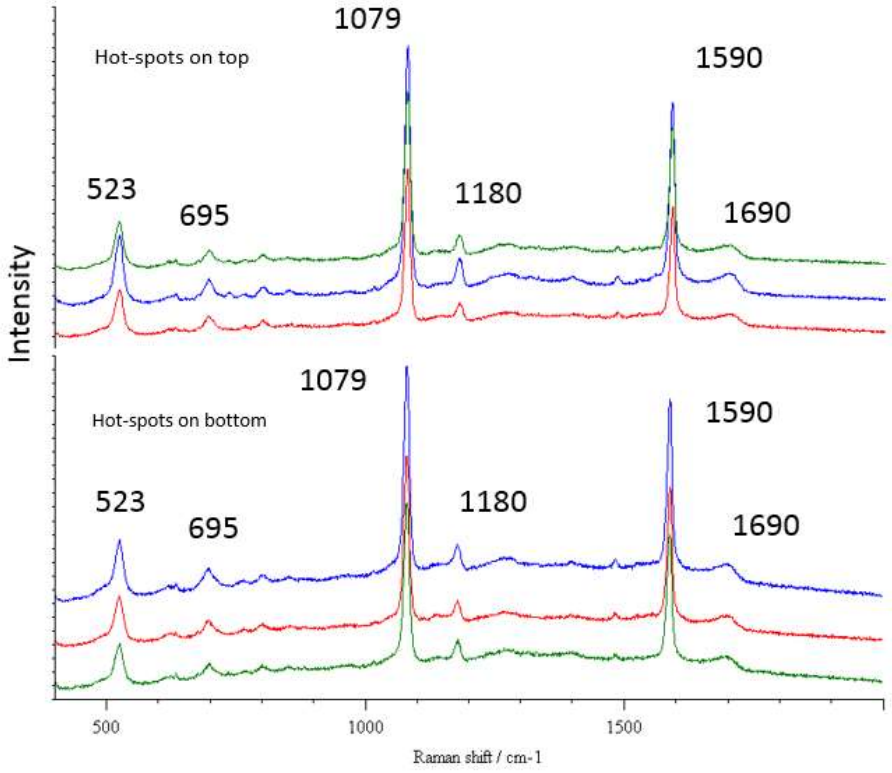

Figure 12. SERS spectrum of 4-MBA SAM taken in situ on three different Q3D-PNAs of each with hot spots at the water/Au interfaces on top and at bottom, respectively.

COS-7 and HepG2 cells studied using SERS microfluidic devices

The cultured COS-7 and HepG2 cells are about 18-20 μm as shown in the optical images in Fig. 13. The size is about one Q3D-PNA pattern. SERS spectra of COS-7 and HepG2 cells taken on three different locations of the same Q3D-PNA with the hot spots on top are shown in Figs. 14 and 15, indicating that Q3D-PNAs has high reproducibility for cell detections. Figure 16 shows the SERS spectra taken from three locations of a Q3D-PNA pattern that was half-covered by a HepG2 cell. The SERS spectrum taken at the cell-uncovered area of the Q3D-PNA has no any obvious peak comparing to those two spectra taken at the cell-covered area, which confirms that all the peaks are from cells. The peak at 490 cm^{-1} represents the

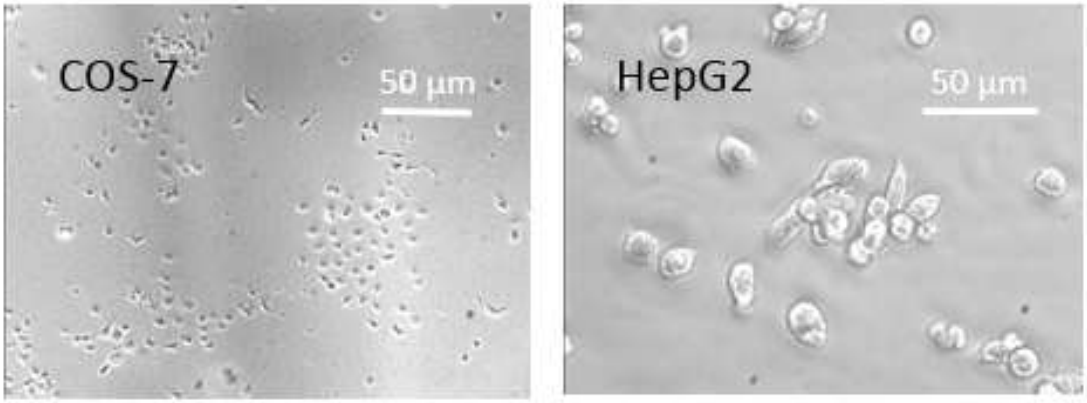

vibration of disulfide bond (S-S). The peak around 680-690 cm^{-1} corresponds to the

vibration of C-S bond. All are related to proteins on cell membranes or cytoplasm. Two peaks at 620 and 1410 cm^{-1} are from the carboxylate (COO-). Peaks of 670, 790 and 812 cm^{-1} are probably from DNA/RNA, indicating that cells in channel were probably broken and the inner cellular objects like cytoplasm or nucleus were out. The strong peak at 715 cm^{-1} could be from Adenine. The peaks located at 1260, 1319 and 1515 cm^{-1} are related to protein amide III.

Figure 13. Optical images of cultured COS-7 and HepG2 cells.

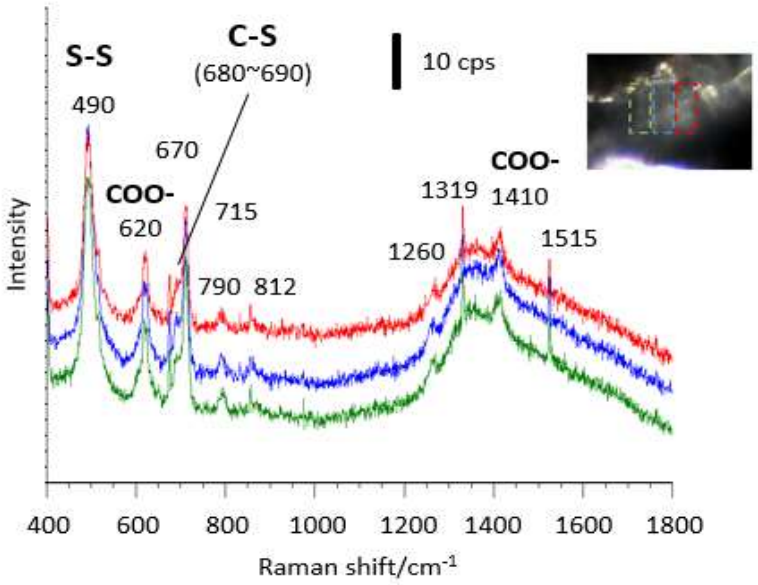

Figure 14. SERS spectra of one COS-7 cell taken at three different locations of one Q3D-PNA with hot spots on top.

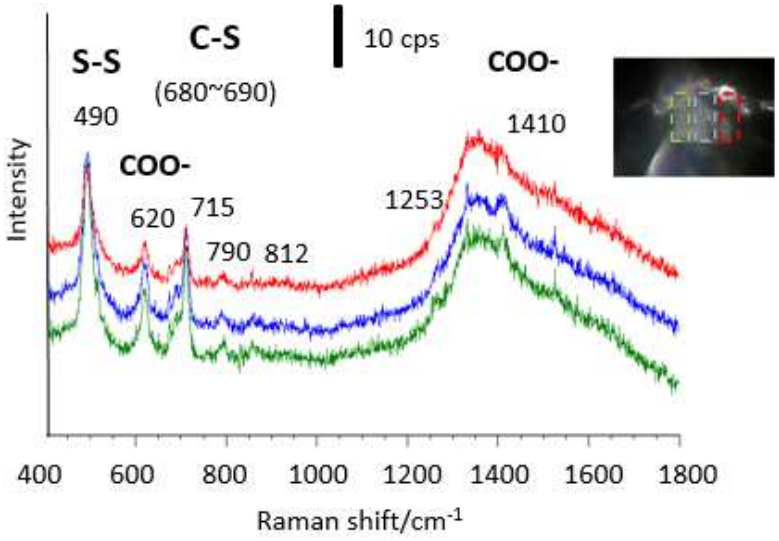

Figure 15. SERS spectra of one HepG2 cell taken at three different locations of one Q3D-PNA with hot spots on top.

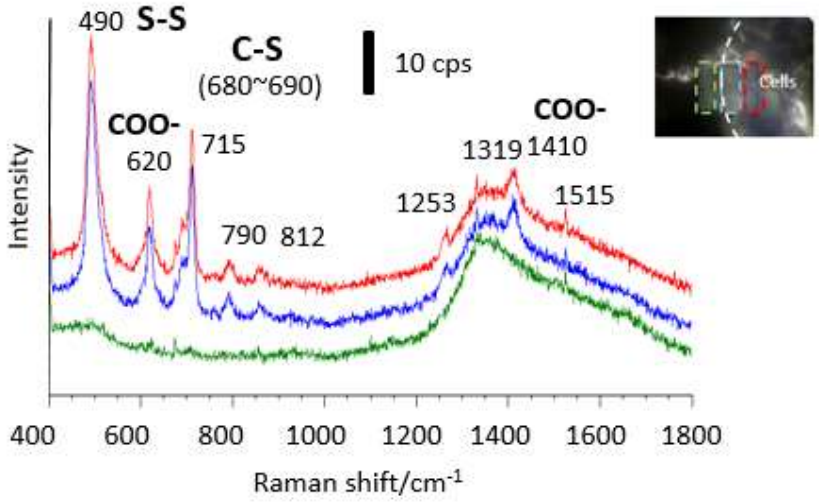

Figure 16. Comparison of SERS spectra taken from three different locations of one Q3D-PNA that is half-covered by a HepG2 cell.

To further confirm SERS signals from cells, more SERS spectra were taken from different locations for comparison. Figure 17 shows the SERS spectra taken on one Q3D-PNA with COS-7 cell and another without COS-7 cells. Clearly, SERS spectrum taken from the Q3D-PNA without cells has no obvious peaks except the broaden one due to glass absorption. Similarly, Figure 18 shows the comparison for

HepG2 cells. The comparison of SERS spectra of HepG2 taken on two types of Q3D-PNAs is shown in Fig. 19A. The Q3D-PNA having hot spots on top yields stronger SERS signals of the cell than that having hot spots at bottom because cells can only attach to the top gold surface of Q3D-PNAs. The SERS spectrum of cells on flat gold surface without Q3D-PNAs was also taken and is shown in Fig. 19B. This demonstrates that the Raman signals of cells are basically invisible without SERS enhancement. Figure 20 compares the SERS spectra of COS-7 and HepG2 with 10 times of accumulation. There is no obvious difference between these two SERS spectra of different cells. Since all these peaks are either related to DNA/RNA or proteins of cytoplasm and nucleus or cell membranes, cells in channels could be broken.

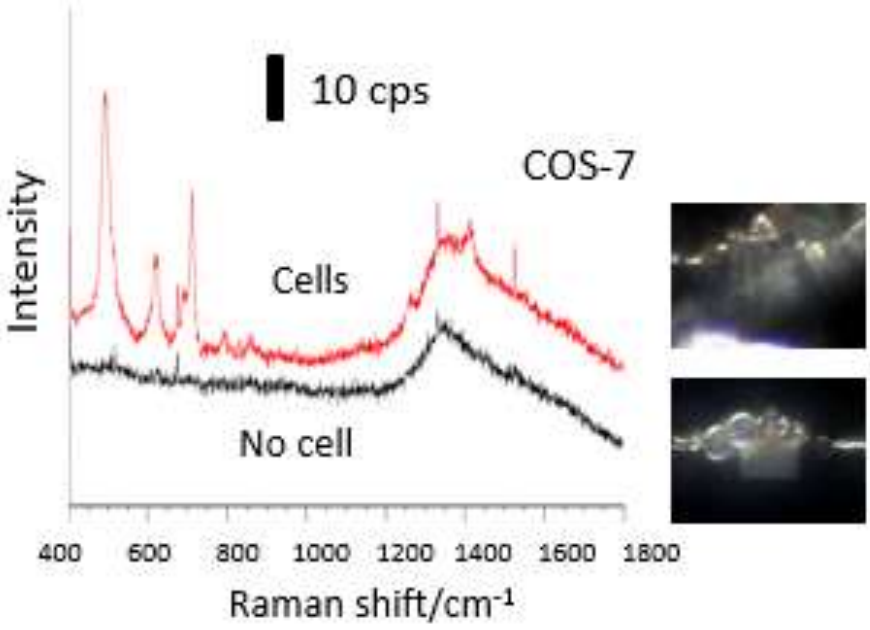

Figure 17. Comparison of SERS spectra in different location. Q3D-PNAs having COS-7 cells attaching v.s. no cell attaching

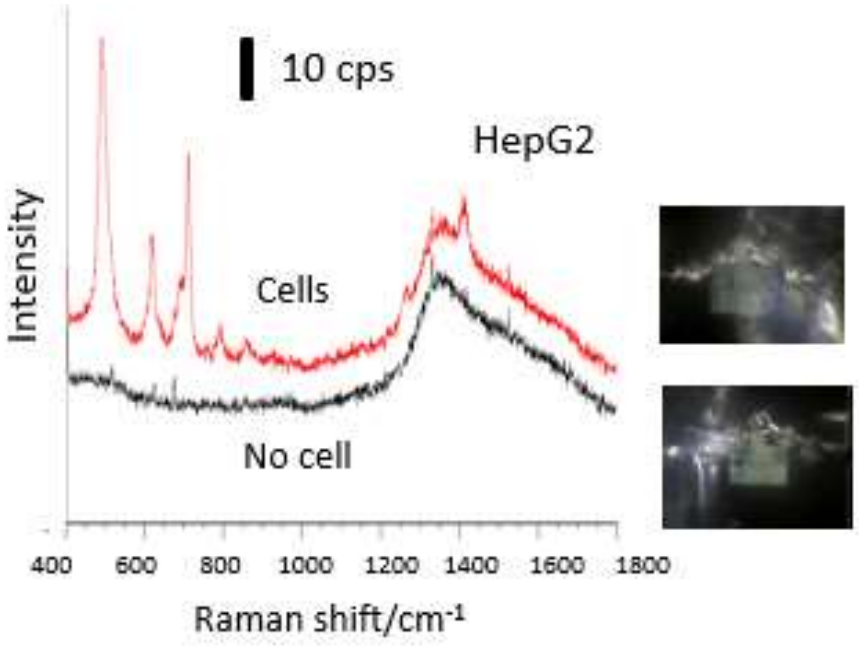

Figure 18. Comparison of SERS spectra in different location. Q3D-PNAs having HepG2 cells attaching v.s. no cell attaching

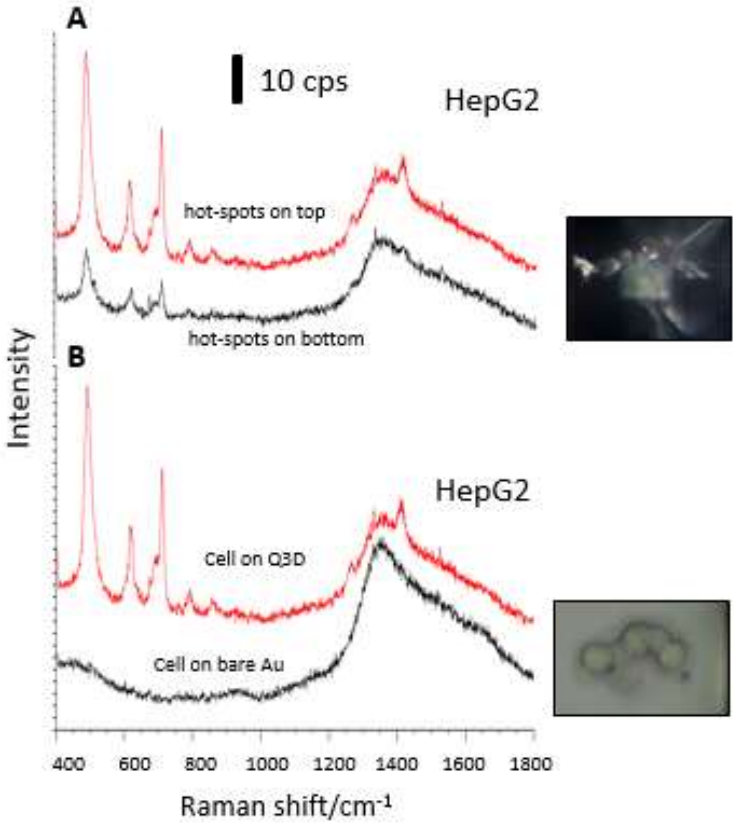

Figure 19. A. HepG2 on Q3D-PNAs with hot-spots on top v.s. on bottom **B.** HepG2 on Q3D-PNAs v.s. no Q3S-PNAs

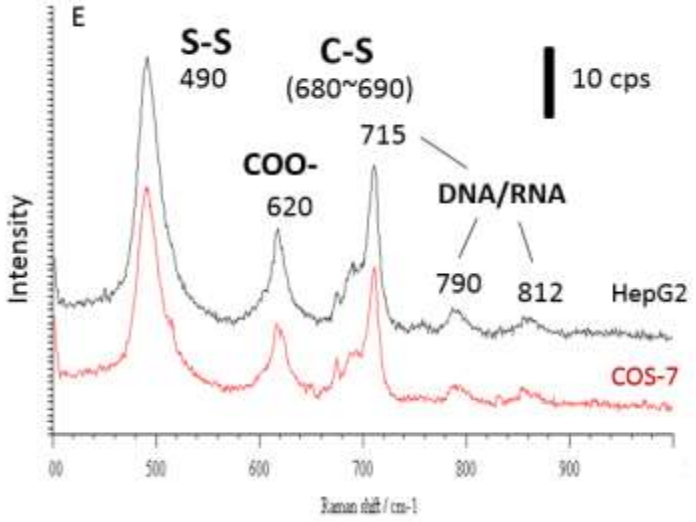

Figure 20. Comparison of SERS spectra of COS-7 and HepG2 cells.

Conclusions

In this work, an h-PDMS/PDMS microfluidic device containing Q3D-PNA SERS-active substrates surrounding with cell traps was designed, fabricated and demonstrated for SERS analysis of cells. The FDTD method presented as an excellent tool for designing the dimensions of Q3D-PNAs with spatial control of the strongest local electric fields. The Q3D-PNAs with hot spots at the water/Au interfaces on top and bottom were designed with the electromagnetic enhancement

factors of $1.15x10^{-5}$ and $3.32x10^{-5}$, respectively.. SERS spectra of 4-MBA taken on Q3D-PNAs after its solution flowing through microfluidic channels demonstrated great efficiency and reproducibility of Q3D-PNAs as SERS-active substrates built in microfluidic channels. With many comparisons of SERS spectra of COS-7 and HepG2 taken on Q3D-PNAs patterns in microfluidic channels, the capability of in-situ cell detection by using SERS-based microfluidic devices was demonstrated.

References

1 Jeanmaire, David L.; Richard P. van Duyne (1977). "Surface Raman Electrochemistry Part I. Heterocyclic, Aromatic and Aliphatic Amines Adsorbed on the Anodized Silver Electrode." Journal of Electroanalytical Chemistry 84: 1–20

2 M. Fleischmann, P.J. Hendra, A.J. McQuillan, Raman Spectra of Pyridine Adsorbed at a Silver Electrode Chemical Physics Letters **26** (2): 163–166.

3 J. Xu, L. Zhang, H. Gong, J. Homola, Q. Yu, Tailoring plasmonic nanostructures for optimal SERS sensing of small molecules and large microorganisms, Small 7 (2011) 371–376.

4 J. Xu, J.W. Turner, M. Idso, S.V. Biryukov, L. Rognstad, H. Gong, V.L. Trainer, M.L.Wells, M.S. Strom, Q. Yu, In situ strain-level detection and identification of vibrio parahaemolyticus using surface-enhanced Raman spectroscopy, Anal. Chem. 85 (2013) 2630–2637.

5 J. Xu, P. Kvasni9cka, M. Idso, R.W. Jordan, H. Gong, J. Homola, Q. Yu, Understanding the effects of dielectric medium substrate, and depth on electric fields and SERS of quasi-3D plasmonic nanostructures, Opt. Express 19 (2011) 20493–20505.

6 Q. Yu, S. Braswell, B. Christin, J. Xu, P.M. Wallace, H. Gong, D. Kaminsky, Surface-enhanced Raman scattering on gold quasi-3D nanostructure and 2D nanohole arrays, Nanotechnology 21 (2010) 355301–355309

7 Y. Deng , M. N. Idso, D. D. Galvan, Q. Yu, Optofluidic microsystem with quasi-3 dimensional gold plasmonic nanostructure arrays for online sensitive and reproducible SERS detection

8 B. Han, N. Choi, K. H. Kim, D. W. Lim, and J. Choo, Application of Silver-coated magnetic microspheres to a SERS-based optofluidic sensor, Journal of Physical Chemistry C, vol. 115, no. 14, pp. 6290–6296, 2011.

9 J. Yang, Z. Wang, S. Zong, C. Song, R. Zhang, Y. Cui, Distinguishing breast cancer cells using surface-enhanced Raman scattering, Anal Bioanal Chem (2012) 402:1093–1100

10 X. Wang, X. Qian, J. J. Beitler, Z. (Georgia) Chen, F. R. Khuri, M. M. Lewis, H. Ju-C. Shin, S. Nie, and D. M. Shin, Detection of Circulating Tumor Cells in Human Peripheral Blood using Surface-Enhanced Raman Scattering Nanoparticles, Cancer Res. 2011 March 1; 71(5): 1526–1532

11 J. P. Scaffidi, M.K. Gregas, V. Seewaldt, T. Vo-Dinh, SERS-based plasmonic nanobiosensing in single living cells, Anal Bioanal Chem. 2009 February ; 393(4): 1135–1141

12 T-Y. Liu, K-T Tsai, H-H Wang, Y. Chen, Y-H Chen, Y-C Chao, H-H Chang, C-H Lin, J-K Wang, Y-L Wang, Functionalized arrays of Raman-enhancing nanoparticles for capture and culture-free analysis of bacteria in human blood, Nature Communications **2**, Article number: 538

13 C. Andreou, M. R. Hoonejani, M. R. Barmi, M. Moskovits, C. D. Meinhart, Rapid Detection of Drugs of Abuse in Saliva Using Surface Enhanced Raman Spectroscopy and Microfluidics, *ACS Nano*, **2013**, *7* (8), pp 7157–7164

14 C.D. Syme, N.M.S. Sirimuthu, S.L. Faleyab, J.M. Cooper, SERS mapping of nanoparticle labels in single cells using a microfluidic chip, Chem. Commun., 2010, **46**, 7921–792

15 J. R. Etzkorn, W.-C. Wu, Z. Tian, P. Kim, S.-H. Jang, D. R. Meldrum, A. K.-Y. Jen, B. A. Parviz, Using Micro-Patterned Sensors and Cell Self-Assembly for Measuring the Oxygen Consumption Rate of Single Cells, J. Micromech. Microeng**.**, 20, 095017, 201

16 S. J. Tan, L. Yobas, G. Y. H. Lee, C. N. Ong, C. T. Lim, Microdevice for the isolation and enumeration of cancer cells from blood, Biomed Microdevices (2009) 11:883–892

17 J. R. Rettig, A. Folch, Large-Scale Single-Cell Trapping And Imaging Using Microwell Arrays, Anal. Chem. **2005,** 77, 5628-5634

18 H. Mohamed, M. Murray, J. N. Turner, M. Caggana, Isolation of tumor cells using size and deformation, Journal of Chromatography A, 1216 (2009) 8289–8295

19 Y. Xia, G. M. Whitesides, Soft lithography, Annu. Rev. Mater. Sci. 1998. 28:153–84

20 Bayu Atmaja, Jane Frommer, J. Campbell Scott, Atomically Flat Gold on Elastomeric Substrate, *Langmuir*, 2006, *22* (10), pp 4734–4740

21 D. Qin, Y. Xia, G. M Whitesides, Soft lithography for micro-and nanoscale patterning, *Nature Protocols* **5**, -491 - 502 (2010)

22 A.R. Halpern, K.C. Donavan, R.M. Penner, R.M. Corn, Wafer-scale fabrication of nanofluidic arrays and networks using nanoimprint lithography and lithographically patterned nanowire electrodeposition gold nanowire masters, Anal. Chem. 84 (2012) 5053–5058

23 A. Michota, J. Bukowska, Surface-enhanced Raman scattering (SERS) of 4-mercaptobenzoic acid on silver and gold substrates, J. Raman Spectrosc. 2003, 34, 21

24 Libin Yang, Xin Jiang, Weidong Ruan, Bing Zhao, Weiqing Xua, John R. Lombardic, Adsorption study of 4-MBA on TiO2 nanoparticles by surface-enhanced Raman spectroscopy, J. Raman Spectrosc. 2009, 40, 2004–2008

25 Jiajie Xu, Pavel Kvasnička, Matthew Idso, Roger W. Jordan, Heng Gong, Jiří Homola, and Qiuming Yu, Understanding the effects of dielectric medium, substrate, and depth on electric fields and SERS of quasi-3D plasmonic nanostructures, Optics Express Vol. 19, Issue 21, pp. 20493-20505 (2011)

26 Marc A. Unger, Hou-Pu Chou, Todd Thorsen, Axel Scherer, Stephen R. Quake, Monolithic microfabricated valves and pumps by multilayer soft lithography, Science April 2000: Vol. 288 no. 5463 pp. 113-116